On Inclusion of Urban Landscape in a Climate Model – How can satellite data help?

Menglin Jin[1] and J. Marshall Shepherd[2]

1. Department of Meteorology, University of Maryland, College park.
mjin@atmos.umd.edu

2. NASA Goddard Space Flight Center Code 912.0, Greenbelt, MD.

January 2004

Urban regions, which cover only approximately 2% of the Earth's land surface, contain about half of the human population (UNPD 2001). Modeling urban weather and climate is critical for human welfare but has been hampered by at least two reasons: (i) no urban landscape has been included in global and regional climate models (GCMs and RCMs), and (ii) detailed information on urban characteristics is hard to obtain. With the advance of satellite observations, adding urban schemes into climate models in order to scale projections of global/regional climate to urban areas becomes essential. Inclusion of urbanized landscape into climate models was discussed in depth at the Fall American Geophysical Union (AGU) meeting of 2003 in the Union session entitled "Human-induced climate variations linked to urbanization: From Observations to Modeling", which took place on December 12, 2003 in San Francisco, USA. The following notes summarizes what is known and what needs to be done on this topic.

In a GCM and RCM, land physical processes are simulated in a land surface model, which is coupled with the atmosphere model through exchanges of heat fluxes, water, and momentum. Currently, an urban classification is not included in any major GCM/RCM's land surface model (for example, the National Center for Atmospheric Research (NCAR) Community Land Model (CLM2), NASA Global Modeling and Assimilation Office (GMAO) unified land surface model, Biosphere-Atmosphere-Transfer Scheme (BATS), SIB2, etc). This exclusion makes GCMs/RCMs inadequate for realistically simulating urban modifications to climate.

The same land surface model can be coupled to a GCM or RCM. For example, the NCAR CLM is coupled to both the NCAR community atmosphere model (CAM) as well as a regional model. Therefore, including urban landscape into a land surface model is the practical way, and probably the only way, to represent urban environments in a GCM or RCM.

1. New Data and Availability

Urbanization is an old topic that can be dated back to the 1800s (Langsberg 1956, Oke 1978). Observations from satellites, with their richness, quality, resolution,

and coverage, provide a new approach for studying urban environments. Among others, NASA's Terra, Aqua, Landsat, and Tropical Rainfall Measuring Mission (TRMM) are especially important satellites for global and regional urban studies. For example, observations from MODIS on Terra and Aqua provide nearly daily global coverage of the Earth in 36 spectral bands at spatial resolutions of 1 km or better (depending on band), four times per day, and with over 40 data products. Both land surface and atmosphere conditions modified by urban environments can now be detected from MODIS. Among others, the most important urban-related variables which can be obtained from MODIS include:

(a) land surface reflectance and albedo
(b) land surface emissivity
(c) leaf area index (LAI)
(d) land surface skin temperature (T_{skin})
(e) land cover
(f) snow coverage
(g) cloud properties
(h) aerosol properties

For urban modeling purposes, three advantages of MODIS data make it extremely valuable:

- First, the instantaneous observations can be used to study the interaction between the land surface and its overlying atmosphere through various variables;

- Second, its global coverage enables observations of all urban pixels over the globe, identification of the extremities and median of urban impacts, and study of the intensity of urban impacts under different climate systems or regions;

- Third, MODIS data, like those from Landsat and ASTER, have promising quality.

MODIS' teams have designed specific validation methods for each product via field *in situ* observations and algorithm inter-comparisons. For example, land surface emissivity is now available for the first time globally. Although uncertainties remain over some areas, this dataset provides both global distribution and seasonal variations. This product, together with emissivity data from ASTER, illustrates urban emissivity variations.

In addition, land cover, LAI, albedo, and skin temperature are globally available. For example, Figure 1a shows the global distribution of land cover classification as derived from MODIS data, with Fig. 1b showing the corresponding distribution of land cover classification in the southeastern US in the vicinity of Atlanta. Furthermore, aerosol optical thickness, cloud optical thickness, and cloud effec-

tive radius can be used to study how urban aerosols change urban cloud microphysics (cf. Figure 2a-c).

Daily and monthly MODIS atmosphere data are accessible from modis- atmosphere.gsfc.nasa.gov. In addition, this site contains the surface albedo, ecosystem classification, and NDVI data derived from global MODIS land data, and filled in for missing data due to persistent cloud cover and seasonal snow. Additional land data are described and available from modis-land.gsfc.nasa.gov. These data can also be ordered through online ftp service and CDs from lpdaac2.usgs.gov/modis/dataproducts.esp.

2. What is urban?

Why do we need to add a new "urban" landscape in land models? Why cannot other land surface types be used to represent urban environments? To answer these questions, we have to know what are the unique physical processes and parameters of urban regions. Satellite observations help identify these features.

With the construction of buildings, parking lots, and houses, urban areas dramatically change the smoothness of a surface (i.e., roughness length), thermal conductivity, hydraulic conductivity, albedo, emissivity, and fraction of vegetation cover. As a result, urban landscapes modify not only the original physical processes that govern any natural land surfaces (i.e., surface energy budget (SEB)), but also add new, unique biogeophysical and biogeochemical processes into land surface-atmosphere, such as storage heat flux, canyon effect, and anthropogenic heat flux. An urban scheme needs to reflect both the modified as well as the new processes.

By measuring spatial variations of urban and non-urban regions, satellite data help distinguish the modified properties that affect SEB, the basis on which a land surface model is built:

$$(1 - a)S\downarrow + LW\uparrow - \varepsilon T_{skin}^4 + SH + LE + G = 0, \quad (1)$$

where SH is sensible heat flux, LE is latent heat flux, and G is the ground heat flux. These three processes compete for surface net radiation R_n, which is the downward minus upward shortwave and longwave radiation. In Eq. (1), a is surface albedo, and $S\downarrow$ is downward solar radiation; therefore $(1 - a)S$ is reflected solar radiation. $LW\uparrow$ is upwelling longwave radiation from the atmosphere near the surface. Emissivity (ε) and surface skin temperature (T_{skin}) determine the upward longwave radiation, or surface emission, following the Stefan-Boltzmann Law. It is evident that decreases of α and ε play important roles in surface temperature changes since input radiative energy are changed in land surface system. In addition, the heights of buildings increase the surface "roughness length" and thus SH and LE are affected by enhanced surface turbulence. Furthermore, urban paved roads and concrete surfaces are waterproof

and thus *LE* tends to be zero over these surfaces.

Figure 3 compares the spectral surface albedo of various land cover classifications in a region of the upper Midwest that includes Chicago and Indianapolis, based on NASA GSFC surface reflectance analysis. Urban land cover has an albedo lower than cropland and broadleaf forests, but higher than needleleaf forests in both the visible and near infrared wavelengths. Since albedo accuracy affects land surface model results, accurate albedo data for urban regions is needed. More information on urban albedo can be found at M. D. King's invited presentation (King 2003).

Figure 4 shows the MODIS measured emissivity for Beijing and surrounding regions. Beijing has a lower emissivity than the surrounding, non-urban regions, with the minimum at 0.935 in the central part of the city. The surrounding regions have an emissivity as high as 0.96-0.97 for normal vegetative areas. The city evidently decreases the emissivity by up to 4%, which may be small in value but large in terms of the thermal properties, since land surface emissivity varies modestly for natural surfaces—0.96-0.97 for vegetation and 0.92-0.95 for most bare soil with extreme low values around 0.8 in deserts. The 4% emissivity decrease implies a big change of land cover, suggesting that the urban environment is indeed a unique land cover classification that should be taken into account in land-surface models as a separate landscape.

Urban landscape significantly affects skin temperature (cf. Fig. 5). The temperature difference of urban and non-urban areas is referred to as the "urban heat island effect" (UHI, Landsberg 1956). Conventionally, UHI was detected from nighttime WMO 2 m surface air temperature records (T_{air}). Satellite data illustrate unique UHI features on T_{skin} as opposed to T_{air}. T_{skin} UHI occurs during the daytime as well as at nighttime, whereas during daytime T_{skin} UHI tends to have a larger intensity than at nighttime. Such unique features are partly due to the physical differences between T_{skin} and T_{air} (Sun and Mahrt1995, Jin et al. 1997), and partly due to the size, density, and microphysics of the city itself. More results of UHI can be found from presentations given by Melisi et. al (2003), Taniguchi et. al. (2003), and Jin and Peters-Lidard (2003).

Satellite T_{skin} data can then be used in two ways for urban modeling: (i) the model output can be directly compared with satellite observations to see if the model reasonably reproduces the size and intensity of UHI, and (ii) satellite-derived T_{skin} can be analyzed to advance our understanding of urban thermal structure, and thus help improve urban parameterizations.

Urban environments change surface vegetation cover as well, which is reflected in a land surface model as LAI and fractional vegetation cover. By replacing original vegetated surface with buildings, roads, or parking lots, LAI and fractional vegetation cover are dramatically reduced. The MODIS LAI product can

provide fine-resolution information between urban and non-urban regions.

Besides land surface, urban areas modify atmospheric conditions. Over urban regions, the aerosol optical thickness can be as high as 0.6 (Figure 2a), which in turn reduces solar insolation by about 30 Wm^{-2} (direct effect). The high concentration of urban aerosol may increase downward longwave radiation partly due to its absorption and emission and partly due to more clouds in the sky.

Aerosol-cloud interactions modify cloud properties, in particular, cloud effective radius and cloud amount, as shown in July 2001 data for the Houston region (Figure 6). The diurnal cycle of cloud properties are observed. From Terra observations during the morning overpass (about local time 10:30 am), the maximum cloud optical thickness occurred at 2.5 with ice particle size of 25 μm, while Aqua observations during the afternoon overpass (about local time 1:30 pm), the ice particle size remained about the same but there were two peaks in cloud optical thickness, one at 2.5 and another at 100. Furthermore, the frequency of clouds in the afternoon was much greater than during the morning.

Recent evidence also suggests that rainfall and subsequent land surface hydrology are also modified by the urban environment (Rosenfeld 1999; Shepherd and Burian 2003). Figure 7 illustrates two MM5-Slab (i.e., a basic land surface model) runs in which the Houston urban surface is included (URBAN) versus not included (NOURBAN). In the NOURBAN run (right hand panel), the urban area is replaced by cropland. In the URBAN case (left hand panel), the apparent high surface temperatures west of Galveston Bay represent the urban heat island. Other features of note include convection west of the UHI that seems to be enhanced and/or forced by an interaction between the sea breeze/outflow boundaries and the boundary of the UHI. There is evidence of a convergence zone associated with the UHI as well. In the NOURBAN run, neither the western convective cluster nor a convergence signature in the wind (near 300 m) is evident. More urban impact on rainfall can be found at presentations given by Rosenfeld et al. (2003), Hooshialsadat et al. (2003), and Wilcox (2003)

3. What do we need for modeling urban regions?

In order to include urban effects in land-surface model, the first objective should be the development of an urban scheme that can be blended into current land surface models.

Roughness length Probably the largest challenge in developing urban schemes is to calculate the roughness length, which is a function of buildings and the combination of various urban surfaces (roads, roofs, trees, etc). Detailed discussion of how to infer roughness length is beyond the scope of this paper, but has been discussed in talks given by R. E. Dickinson (Dickinson 2003) and S. Grimmond (Grimmond 2003).

Urban geometry database

To calculate roughness length, we need urban building information. Global urban building density, coverage, and height information is important but not yet available. One prototype data set of such was developed by Steve Burian of the University of Utah for the Houston area. His urban database includes multiple surface topography and surface cover datasets, via GIS. Urban canopy parameters are given in Table 1.

Table 1. Urban canopy parameters.

	Urban Canopy Parameter
1	Mean Building Height
2	Standard Deviation of Building Height
3	Mean Building Height Weighted by Footprint Plan Area
4	Wall-to-Plan Area Ratio
5	Building Height-to-Width Ratio (λ_s)
6	Building Height Histograms
7	Mean Vegetation Height Weighted by Plan Area
8	Mean Canopy Height Weighted by Plan Area
9	Mean Orientation of Street
10	Building Plan Area Density Function ($A_{pb}(z)$)
11	Vegetation Plan Area Density Function ($A_{pv}(z)$)
12	Canopy Plan Area Density Function ($A_{pc}(z)$)
13	Building Rooftop Area Density Function ($A_{tb}(z)$)
14	Vegetation Top Area Density Function ($A_{tv}(z)$)
15	Canopy Top Area Density Function ($A_{tc}(z)$)
16	Building Frontal Area Density Function ($A_{fb}(z)$)
17	Vegetation Frontal Area Density Function ($A_{fv}(z)$)
18	Canopy Frontal Area Density Function ($A_{fc}(z)$)
19	Roughness Length and Displacement Height (Raupach (1994))
20	Roughness Length and Displacement Height (Macdonald (1998))
21	Roughness Length and Displacement Height (Bottema (1997))
22	Sky View Factor
23	Plan Area Fraction of Vegetation, Buildings, Water, Bare Soil, Artificial Surfaces
24	Building Material
25	Directly Connected Impervious Area (DCIA)

(Burian et al. 2003).

Updated urban cover database

The rapid increase in city size requires modelers to have an accurate global urban coverage database. The standard MODIS land cover data set defines the urban coverage based on the Digital Chart of the World, which dates back to the 1960s. Annemarie Schneider and Mark Friedl of Boston University have been working on developing an updated urban land cover database using MODIS pixel radi-

ance, cloud cover, and city lights (see more on Schneider et al. 2003a, b).

4. Final Remarks

Urban schemes are currently being developed for land surface models (Jin and Peters-Lidard 2003, Dickinson 2003). The urban schemes need to include potential feedbacks to the atmosphere and hydrological cycles. Three specific emphases are need to be under considerations: (i) large fraction of impervious (mostly black) surfaces that impact surface temperatures and hydrology, (ii) urban plants—either more or less than natural background—may be irrigated, and (iii) turbulent transports generated by buildings and vegetation at multiple heights.

In conclusion, satellite-observed urban information is extremely useful for advancing our ability of simulating urban effects in climate models. Specifically, satellite data can help us understand the diurnal, seasonal, and interannual variations of urban surface. In addition, satellite data can specify surface parameters for a land surface model and validate the model performance.

REFERENCES

Burian, S.J., Han, W.S., Velugubantla, S.P., and Maddula, S.R.K. (2003). Development of gridded fields of urban canopy parameters for Models-3/CMAQ/MM5. Final Report Prepared for Jason Ching of the U.S. Environmental Protection Agency. Department of Civil & Environmental Engineering, University of Utah, Salt Lake City, UT.

Chu, D., L Remer, J Szykman, Y Kaumfan, D Neil, B Pierce, 2003: Monitoring PM2.5 from Space. Oral Presentation at AGU Fall Meeting.
http://www.meto.umd.edu/~mjin/AGU03urban/ under "Meeting Presentations"

Dickinson, R. E., 2003: Framework for Inclusion of Urbanized Landscapes in a Climate Model. Invited talk at AGU Fall Meeting.
http://www.meto.umd.edu/~mjin/AGU03urban/ under "Meeting Presentations"

Grimmond, S. and T. R. Oke, 2003: Surface-atmosphere exchanges in urban areas: Observations and models. Oral presentation at AGU Fall Meeting.

Hooshialsadat, P., S J Burian, J M Shepherd, 2003: Assessing Urbanization Impact on Long-term Rainfall Trends in Houston. Oral Presentation at AGU Fall Meeting.
http://www.meto.umd.edu/~mjin/AGU03urban/ under "Meeting Presentations"

Jin, M., R. E. Dickinson, and A. M. Vogelmann, 1997: A comparison of CCM2-BATS skin temperature and surface-air temperature with satellite and surface observations.

Jin, M., C Peters-Lidard, 2003: Detecting and Simulating Urban-induced Climate Changes via EOS observations and NCAR Community Land Model. Oral presentation at AGU Fall Meeting.

http://www.meto.umd.edu/~mjin/AGU03urban/ under "Meeting Presentations"

Jin, M. R. E. Dickinson, and D. Zhang, 2004: The footprint of urban areas on global climate as characterized by MODIS. In press by J. of Climate.

King, M., 2003: Promise and Capability of NASA's Earth Observing System to Monitor Human-Induced Climate Variations. Invited talk at AGU Fall meeting, http://www.meto.umd.edu/~mjin/AGU03urban/ under "Meeting Presentations"

Landsberg, H. E., 1973: The climate of town in man's role in changing the face of the Earth. The University of Chicago Press, 584-606.

Milesi, C., C D Elvidge, R R Nemani, S W Running, 2003: Synergistic use of MODIS and Night-time DMSP/OLS Data for the Assessment of the Climatic Effects of Urbanization. Poster presentation at AGU Fall Meeting.
http://www.meto.umd.edu/~mjin/AGU03urban/ under "Meeting Presentations"

Oke, T. R. 1973: City size and the urban heat island. *Atmospheric Environment* **7**: 769-779.

Rosenfeld, D., 1999: TRMM observed first direct evidence of smoke from forest fires inhibiting rainfall. *Geophys. Res. Lett.*, **26**, 3105-3108.

Rosenfeld, D., A Givati, A Khain, G Kelman, 2003: Urban Aerosol-Induced Changes of Precipitation Invited talk at AGU Fall meeting, http://www.meto.umd.edu/~mjin/AGU03urban/ under "Meeting Presentations"

Schneider, A., M. A. Friedl, C. E. Woodcock, 2003a: Synergistic use of MODIS and Nighttime DMSP/OLS Data for the Assessment of the Climatic Effects of Urbanization. Poster presentation at AGU Fall Meeting.
http://www.meto.umd.edu/~mjin/AGU03urban/ under "Meeting Presentations".

Schneider, A., M. A. Friedl, D. K. McIver and C. E. Woodcock, 2003:b Mapping urban areas by fusing multiple sources of coarse resolution remotely sensed data. *Photogramm. Eng. Remote Sens*., **69**, 13771386.

Shepherd, M. J. and S. J. Burian 2003: Detection of urban-induced rainfall anomalies in a major costal city. *Earth Interaction*, **7** (6).

Sun, J. and L. Mahrt, 1995: Determination of surface fluxes from the surface radiative temperature. *J. Amtos. Sci.* **52**, 1096-1106.

Taniguchi, M, Y Sakura, T Uemura, 2003: Effects of urbanization and global warming on subsurface temperature in the three mega cities in Japan. Oral Presentation at AGU Fall Meeting
http://www.meto.umd.edu/~mjin/AGU03urban/ under "Meeting Presentations"

UNPD, 2001: United Nations Population Division World Urbanization Prospects: The 2001 Revision. http://www.un.org/esa/population/publications/wup2001

Wilcox, E. M., 2003: Instantaneous Rain Rates in Satellite Observations and a General Circulation Model. Poster presentation at AGU Fall Meeting.
http://www.meto.umd.edu/~mjin/AGU03urban/ under "Meeting Presentations".

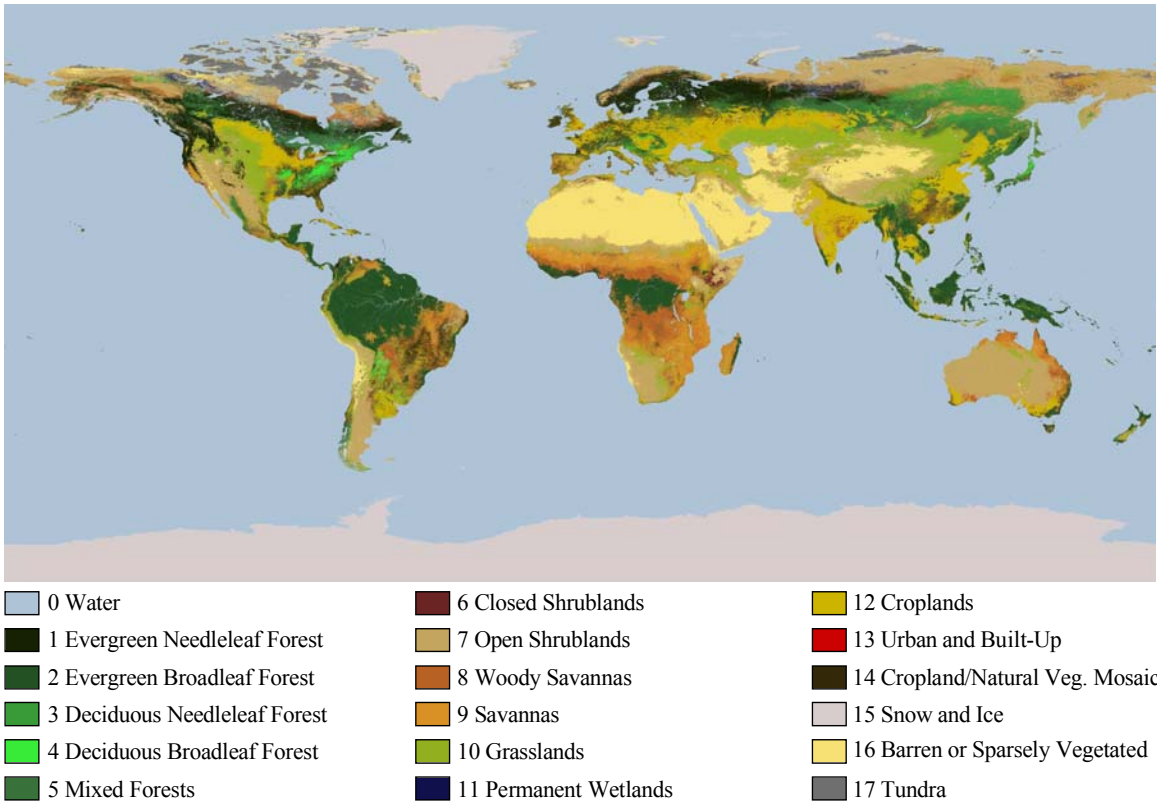

Figure 1a. MODIS land cover classification.

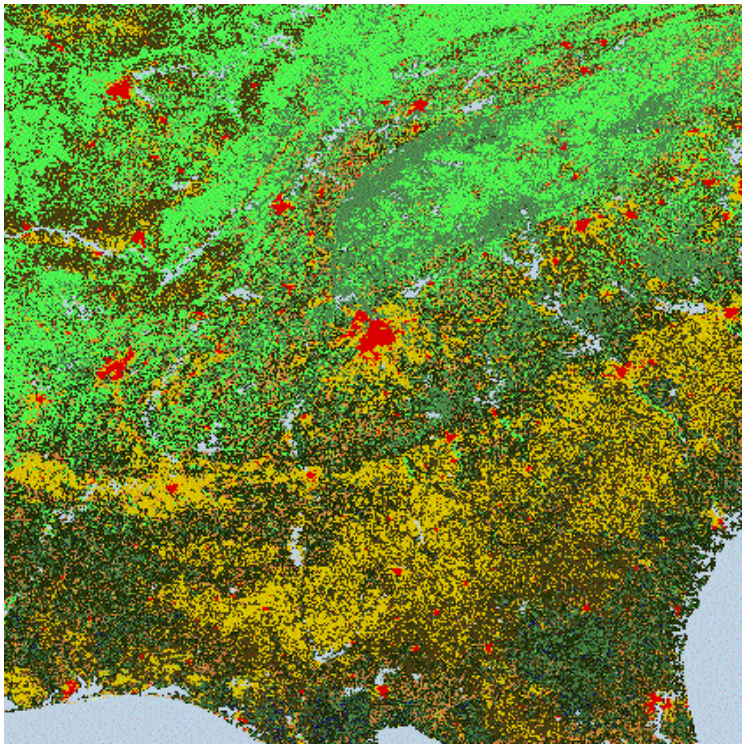

Figure 1b. MODIS land cover classification in southeastern US (near Atlanta). Red color is for Urban and Build-up (land cover classification 13 in Fig. 1b, provide by King (2003))

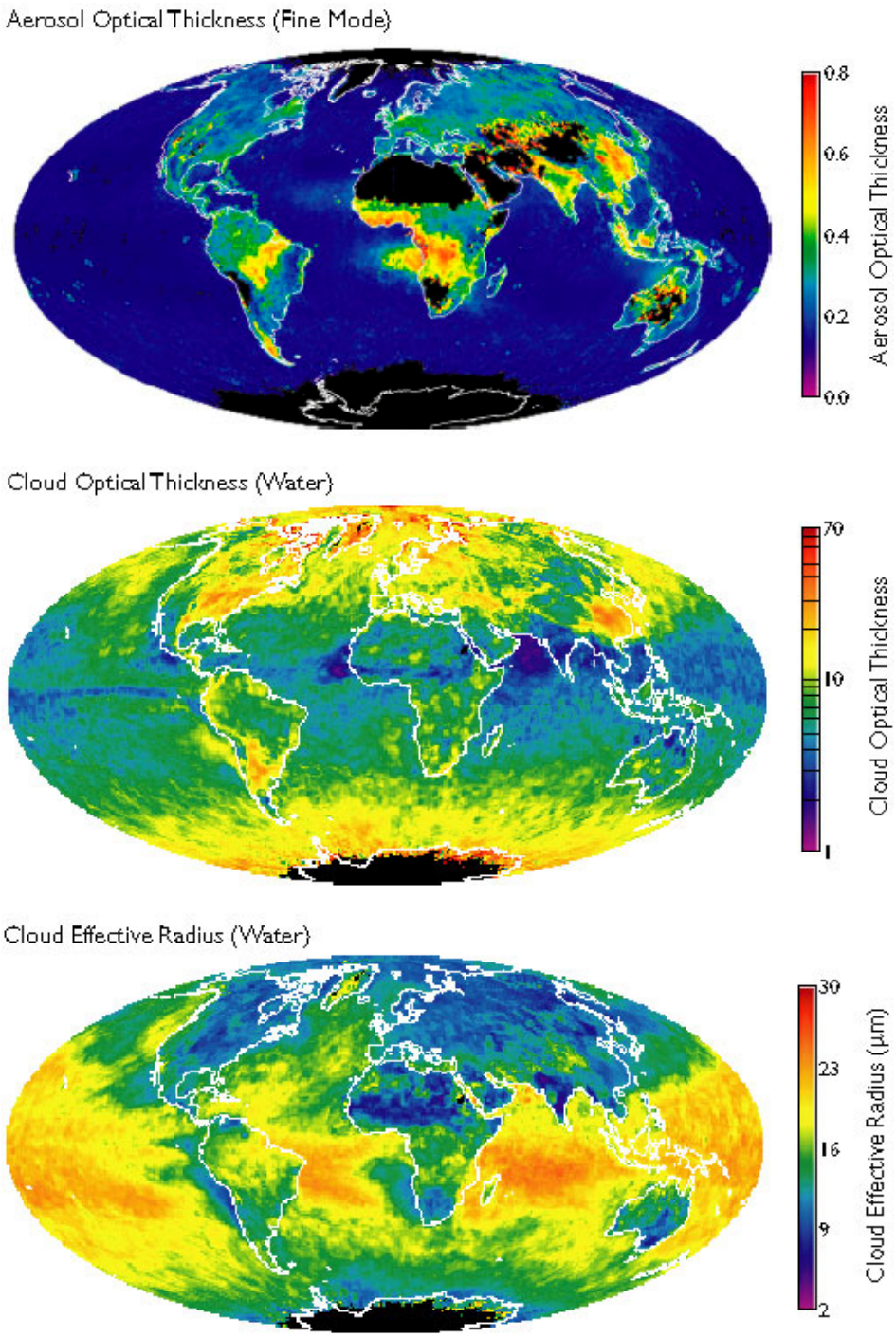

Figure 2 (a) Global distribution of fine aerosol optical thickness derived from MODIS measurements on the Terra platform for September 2000. The large values over Southeast Asia, Indian, Europe and the Unites States reflect urban pollution. The large values in the Southern Hemisphere are due to biomass burning. (b) Global distribution of cloud optical thickness for water clouds from Terra/MODIS on April 2003. (c) same as (b) except for effective radius. (Data obtained from M. D. King of NASA Goddard Space Flight Center). See more on King (2003).

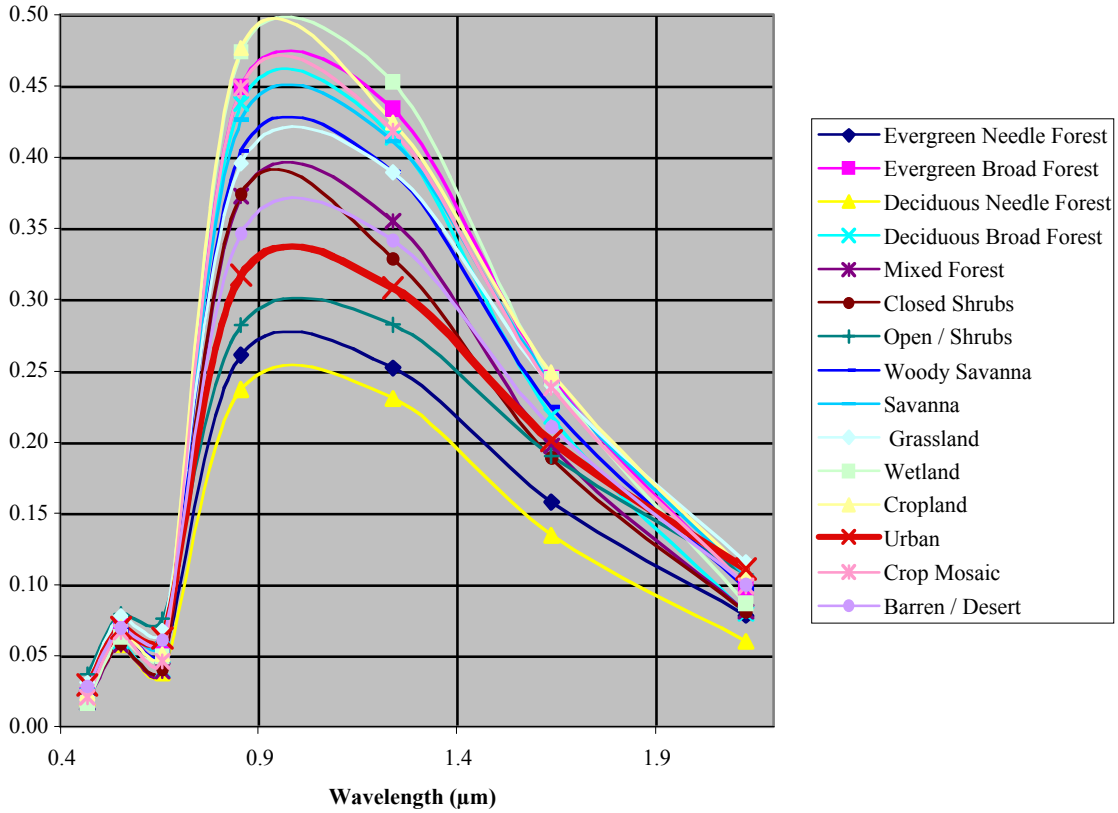

Figure 3. The spectral distribution of reflectance for various land cover types over the upper Midwest at the end of July 2001. Urban is in red line. It shows that urban landscape has lower albedo than cropland and higher than forests over most wavelengths. Urban albedo has evident seasonality, with large value at summer and minimum at winter (not shown). Analysis provided by E. G. Moody and M. D. King, Goddard Space Flight Center. See more on King (2003).

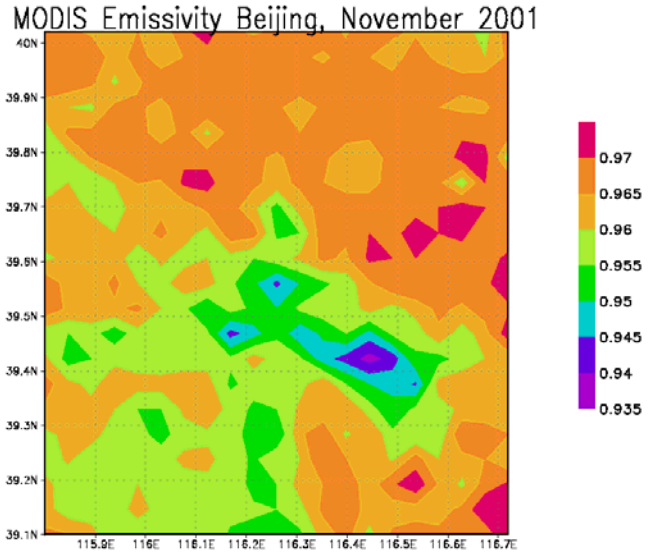

Figure 4. Surface emissivity for Beijing and surrounding regions. The low center of emissivity corresponds to the central part of Beijing. (Provided by Jin.)

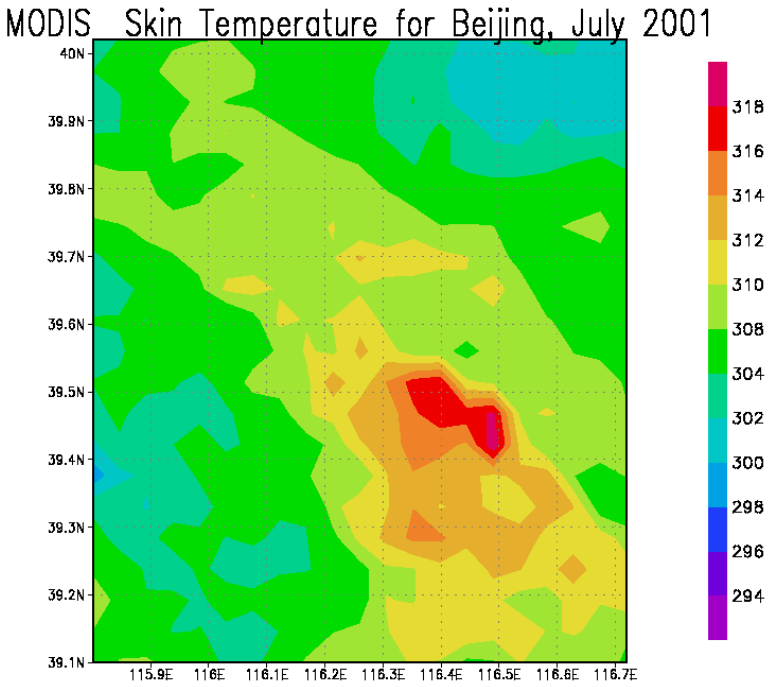

Figure 5. Skin temperature for Beijing and surrounding regions. The high temperature center corresponds to the central part of Beijing. Data is for daytime. (Provided by Jin and Peters-Lidard, (2003), after Jin et. al. 2004).

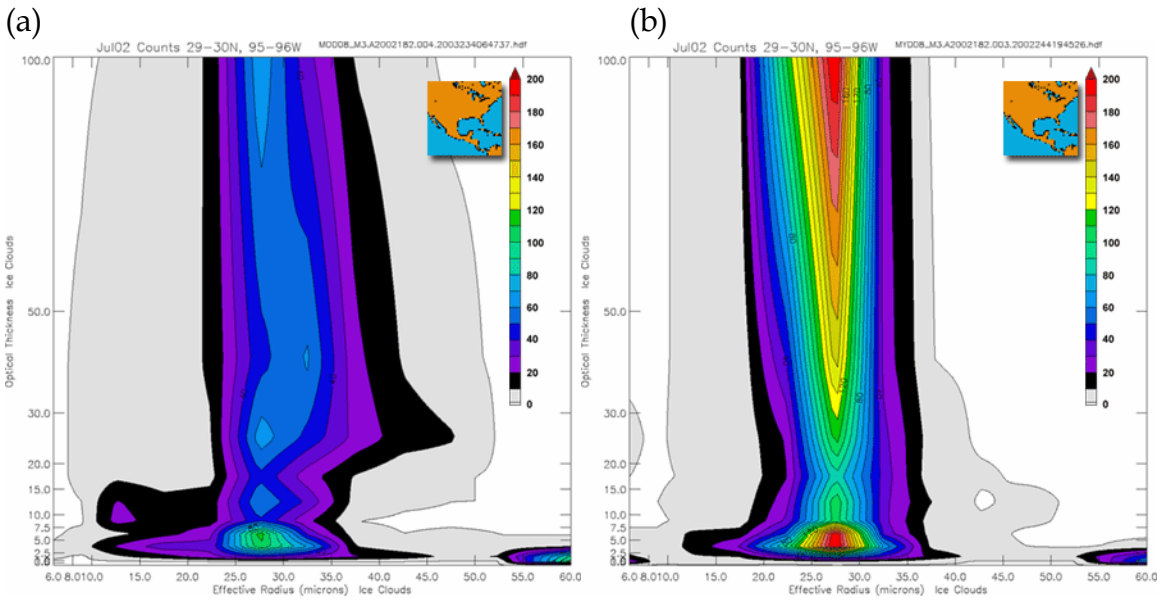

Figure 6. Cloud optical thickness vs. effective radius for water clouds (a) from Terra MODIS (AM overpass) and (b) from Aqua MODIS (PM overpass). (Provided by P. A. Hubanks and M. D. King, Goddard Space Flight Center).

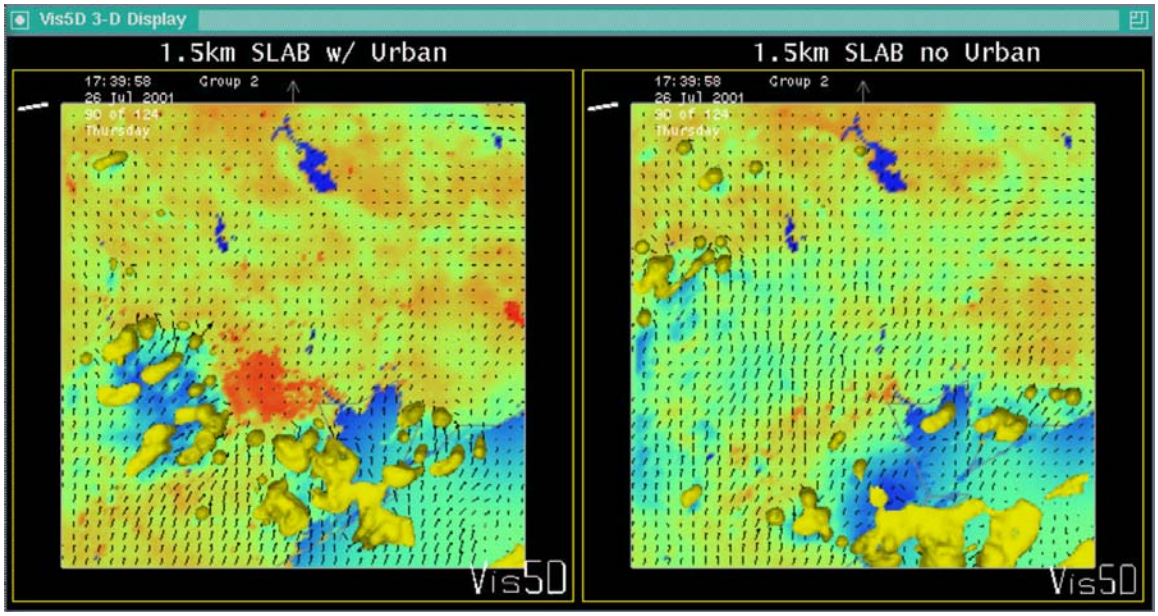

Figure 7. Regional climate model simulated wind, surface temperature, and convective rainfall (yellow) for HOUSTON regions. The left panel is with urban case, and the right panel is without-urban case. (Provided by Shepherd).